# DRAG FORCE ON A CYLINDER EXERTED BY THE CREEPING FLOW OF A GENERALIZED NEWTONIAN FLUID*

RYO NAKAMURA, NAOYA YOSHIOKA AND MASAHIRO MAEDA
*Department of Chemical Engineering, Kyoto University, Kyoto.*

## Introduction

It is found that the Stokes and the Oseen approximations of the Naviear-Stokes equation are very useful for dealing with the creeping flow around an object. When fluid is unbounded in its extent, the ratio of the inertia to the viscous term of this equation becomes larger as the distance from the object increases.

For the case of a sphere, the ratio of the inertia to the viscous term, i. e., the local Reynolds number, at a point in a space is calculated[3] as $V_\infty r/\nu$. This shows that the Stokes assumption is violated at the point where $V_\infty r/\nu = 0(1)$. However, if $Re$ based on the diameter of a sphere is very small compared with 1, one can obtain the uniform approximation to the velocity distribution using the Stokes approximation[6].

On the other hand, for the two dimensional creeping flow perpendicular to the axis of a cylinder infinite in length, the Stokes approximation gives no solution which satisfies both the boundary conditions at the cylinder surface and at the infinity. The solution which satisfies only the former and diverges least rapidly as $r \to \infty$ is of the order of $\ln r$ for the large value of $r$[1], and the velocity distribution obtained from the Stokes approximation contains one undeterminate coefficient. In general, two dimensional creeping flow must be analyzed on the base of the Oseen approximation even if $Re \ll 1$. But when one needs the velocity distribution only in the region near the cylinder, for example, in order to calculate the drag force on it, the solution obtained from the Stokes approximation would be sufficient if one can determine the undeterminate coefficient by an appropriate method.

The asymptotic formula of Lamb's solution[3] of the Oseen equation in the region near the cylinder is very similar to that of the undeterminate solution obtained from the Stokes approximation[6]. It is suggested as an approximation to determine the undeterminate coefficient by comparing these two formulas. The asymptotic solution obtained by this method which is only applicable in the region near the cylinder include the effect of the inertia of fluid, though it is completely neglected in the original Stokes approximation.

Bearing the foregoing in mind, the creeping flow of a generalized Newtonian fluid around a circular cylinder is analyzed approximately by the perturbation method. As is for the case of a sphere[8], the initial term of the expansion reduces to the equation of motion of Newtonian fluid. Strictly, this term must be solved on the base of the Oseen equation. But it is very difficult to solve the first order term of the perturbation parameter by using this result. Since we are concerned only with the asymptotic behavior in the region near the cylinder, the Stokes approximation is adopted and the undeterminate coefficient is determined by the previously mentioned method. Furthermore, in solving the first order term of the perturbation parameter, the boundary condition at the infinity for the perturbed velocity is replaced by the requirment that for the large value of $r$ the solution of the first term is lower order than that of the initial term. The solution thus obtained is not the uniform approximation to the velocity distribution, however it may be considered to be sufficient for the determination of the drag force on a cylinder.

With an attempt to compare the calculated drag force with the experimental data, a circular cylinder was allowed to fall perpendicular to its axis through aqueous solutions of C. M. C. (Carboxymethyl celullose) contained in the rectangular cylinder, and the drag force was determined from the terminal velocity of it.

Generally, for the two dimensional creeping flow, the order of the controling term for the large value of $r$ is $\ln r$, as a consequence, the wall effect is enormously larger than that for three dimensional flow. Therefore we could not carry out the experiment at the condition free from the wall effect. But the interesting result that the drag force is determined only by the zero-shear viscosity was verified experimentally.

## 1. Equation of Motion

Cylindrical coordinates $(r, \theta, Z)$ are chosen with the origin at the axis of the cylinder, $\theta=0$ in the down-stream direction, and $Z$ in the direction of the cylinder axis. Using the Stokes approximation, equations of motion for the steady, incompressible creeping flow become

$$0 = -\frac{\partial P}{\partial r} + \frac{1}{r}\frac{\partial}{\partial r}(r\tau_{rr}) + \frac{1}{r}\frac{\partial \tau_{r\theta}}{\partial \theta} - \frac{\tau_{\theta\theta}}{r}$$

$$0 = -\frac{1}{r}\frac{\partial P}{\partial \theta} + \frac{1}{r^2}\frac{\partial}{\partial r}(r^2\tau_{r\theta}) + \frac{1}{r}\frac{\partial \tau_{\theta\theta}}{\partial \theta} \qquad (1)$$

and equation of continuity is

$$\frac{1}{r}\frac{\partial}{\partial r}(rV_r) + \frac{1}{r}\frac{\partial V_\theta}{\partial \theta} = 0 \qquad (2)$$

Boundary conditions are,

$$\text{B. C. 1.} \quad V_r = V_\theta = 0 \quad \text{at} \quad r = a \qquad (3)$$

* Received on May 25, 1967

B. C. 2. $V_r = V_\infty \cos\theta, \quad V_\theta = -V_\infty \sin\theta$ at $r=\infty$ (4)

Here, $P$ is the pressure,, $\tau_{ij}$ ($i, j=r, \theta$) is the component of the shear stress tensor, and $V_i$ ($i=r, \theta$) is the component of the velocity vector.

For a generalized Newtonian fluid, the relation between the stress tensor and the rate-of-deformation tensor is expressed in the following form,

$$\tau_{ij} = 2\eta_a(\Pi^*)D_{ij} \tag{5}$$

For the low shear rate region, an apparent viscosity $\eta_a$ is approximated by the following equation,

$$\eta_a(\Pi^*) = \frac{\eta_1}{1+\lambda_1^2\Pi^*} + \frac{\eta_2}{1+\lambda_2^2\Pi^*} = \eta_1\left[\frac{1}{1+\varepsilon_1\Pi} + \frac{\alpha}{1+\varepsilon_2\Pi}\right] \tag{6}$$

where

$$\alpha = \frac{\eta_2}{\eta_1}, \quad \varepsilon_i = \lambda_i^2\left(\frac{V_\infty}{a}\right)^2, \quad \Pi = \left(\frac{a}{V_\infty}\right)^2\Pi^*$$

$\Pi^*$ is the second invariant of the rate-of-deformation tensor. That is, $\Pi^*=2D_{ij}D_{ji}$, $D_{ij}=1/2(V_{i,j}+V_{j,i})$ (summation convention is applied for the repeated suffix, and "," denotes the covariant derivative). When an apparent viscosity is approximated by Eq. (6), generally,

$$\alpha<1, \quad \varepsilon_1 \leqslant \varepsilon_2$$

and the value of the second term of the right-hand side of this equation is very small compared with that of the first one. It may be considered that $\eta_a$ is little affected if the second term is approximated in terms of $h(\xi, \theta)$ calculated from the Stokes solution in the following way,

$$\eta_a = \frac{\eta_1}{1+\varepsilon_1\Pi}[1+\alpha h(\xi, \theta)]$$
$$h(\xi, \theta) = 1 - \left(\frac{a}{V_\infty}\right)^2\left(\frac{1}{2A}\right)^2\Pi_{\text{STOKES}} = 1-(\xi^{-1}-\xi^{-3})^2\cos^2\theta - \xi^{-6}\sin^2\theta$$
$$\xi = \frac{r}{a} \tag{7}$$

where $A$ is the undeterminate coefficient which must be determined from the solution of the Oseen equation.

Introducing the following dimensionless quantities,

$$v_i = \frac{V_i}{V_\infty}, \quad \xi = \frac{r}{a}, \quad p = \frac{P}{\eta_1\left(\frac{V_\infty}{a}\right)}$$

it is assumed that $v_i$ and $p$ can be expressed as a power series in $\alpha$ and $\varepsilon_1$ as follows,

$$v = v_0(\xi, \theta) + \alpha v_\alpha(\xi, \theta) + \varepsilon_1 v_\varepsilon(\xi, \theta) + \cdots$$
$$p = p_0(\xi, \theta) + \alpha p_\alpha(\xi, \theta) + \varepsilon_1 p_\varepsilon(\xi, \theta) + \cdots \tag{8}$$

Substituting Eq. (8) into Eqs. (1), (5) and (6), and equating like power of $\alpha$ and $\varepsilon_1$, one obtains a set of differential equation. To the first order in $\alpha$ and $\varepsilon_1$, these equations are expressed as follows.

(i) **Initial term**

$$0 = -\frac{\partial p_0}{\partial\xi} + \left[\nabla^2 v_{r0} - \frac{v_{r0}}{\xi^2} - \frac{2}{\xi^2}\frac{\partial v_{\theta 0}}{\partial\theta}\right]$$
$$0 = -\frac{1}{\xi}\frac{\partial p_0}{\partial\theta} + \left[\nabla^2 v_{\theta 0} - \frac{v_{\theta 0}}{\xi^2} + \frac{2}{\xi^2}\frac{\partial v_{r0}}{\partial\theta}\right] \tag{9}$$

here,

$$\nabla^2 \equiv \frac{1}{\xi}\frac{\partial}{\partial\xi}\left(\xi\frac{\partial}{\partial\xi}\right) + \frac{2}{\xi^2}\frac{\partial^2}{\partial\theta^2}$$

(ii) **First order term in $\alpha$**

$$0 = -\frac{\partial p_\alpha}{\partial\xi} + \left[\nabla^2 v_{r\alpha} - \frac{v_{r\alpha}}{\xi^2} - \frac{2}{\xi^2}\frac{\partial v_{\theta\alpha}}{\partial\theta}\right] + h(\xi, \theta)\left[\nabla^2 v_{r0} - \frac{v_{r0}}{\xi^2} - \frac{2}{\xi^2}\frac{\partial v_{\theta 0}}{\partial\theta}\right]$$
$$+ 2\left(\frac{\partial v_{r0}}{\partial\xi}\right)\frac{\partial h}{\partial\xi} + \left\{\xi\frac{\partial}{\partial\xi}\left(\frac{v_{\theta 0}}{\xi}\right) + \frac{1}{\xi}\frac{\partial v_{r0}}{\partial\theta}\right\}\frac{1}{\xi}\frac{\partial h}{\partial\theta}$$
$$0 = -\frac{1}{\xi}\frac{\partial p_\alpha}{\partial\theta} + \left[\nabla^2 v_{\theta\alpha} - \frac{v_{\theta\alpha}}{\xi^2} + \frac{2}{\xi^2}\frac{\partial v_{r\alpha}}{\partial\theta}\right] + h(\xi, \theta)\left[\nabla^2 v_{\theta 0} - \frac{v_{\theta 0}}{\xi^2} + \frac{2}{\xi^2}\frac{\partial v_{r0}}{\partial\theta}\right]$$
$$+ \left\{\xi\frac{\partial}{\partial\xi}\left(\frac{v_{\theta 0}}{\xi}\right) + \frac{1}{\xi}\frac{\partial v_{r0}}{\partial\theta}\right\}\frac{\partial h}{\partial\xi} + 2\left(\frac{1}{\xi}\frac{\partial v_{\theta 0}}{\partial\theta} + \frac{1}{\xi}v_{r0}\right)\frac{1}{\xi}\frac{\partial h}{\partial\theta} \tag{10}$$

(iii) **First order term in $\varepsilon_1$**

$$0 = -\frac{\partial p_\varepsilon}{\partial\xi} + \left[\nabla^2 v_{r\varepsilon} - \frac{v_{r\varepsilon}}{\xi^2} - \frac{2}{\xi^2}\frac{\partial v_{\theta\varepsilon}}{\partial\theta}\right] - \Pi_0\left[\nabla^2 v_{r0} - \frac{v_{r0}}{\xi^2} - \frac{2}{\xi^2}\frac{\partial v_{\theta 0}}{\partial\theta}\right]$$
$$- 2\left(\frac{\partial v_{r0}}{\partial\xi}\right)\frac{\partial\Pi_0}{\partial\xi} - \left\{\xi\frac{\partial}{\partial\xi}\left(\frac{v_{r0}}{\xi}\right) + \frac{1}{\xi}\frac{\partial v_{r0}}{\partial\theta}\right\}\frac{1}{\xi}\frac{\partial\Pi_0}{\partial\theta}$$
$$0 = -\frac{1}{\xi}\frac{\partial p_\varepsilon}{\partial\theta} + \left[\nabla^2 v_{\theta\varepsilon} - \frac{v_{\theta\varepsilon}}{\xi^2} + \frac{2}{\xi^2}\frac{\partial v_{r\varepsilon}}{\partial\theta}\right] - \Pi_0\left[\nabla^2 v_{\theta 0} - \frac{v_{\theta 0}}{\xi^2} + \frac{2}{\xi^2}\frac{\partial v_{r0}}{\partial\theta}\right]$$
$$- \left\{\xi\frac{\partial}{\partial\xi}\left(\frac{v_{\theta 0}}{\xi}\right) + \frac{1}{\xi}\frac{\partial v_{r0}}{\partial\theta}\right\}\frac{\partial\Pi_0}{\partial\xi} - 2\left(\frac{1}{\xi}\frac{\partial v_{\theta 0}}{\partial\theta} + \frac{v_{r0}}{\xi}\right)\frac{1}{\xi}\frac{\partial\Pi_0}{\partial\theta} \tag{11}$$

here,

$$\Pi_0 = 2\left[\left(\frac{\partial v_{r0}}{\partial\xi}\right)^2 + \left(\frac{1}{\xi}\frac{\partial v_{\theta 0}}{\partial\theta} + \frac{v_{r0}}{\xi}\right)^2\right] + \left[\xi\frac{\partial}{\partial\xi}\left(\frac{v_{\theta 0}}{\xi}\right) + \frac{1}{\xi}\frac{\partial v_{r0}}{\partial\theta}\right]^2$$

Equations of continuity are

$$\frac{1}{\xi}\frac{\partial}{\partial\xi}(\xi v_i) + \frac{1}{\xi}\frac{\partial v_{\theta i}}{\partial\theta} = 0, \quad i = 0, \alpha, \varepsilon_1 \tag{12}$$

## 2. Approximate Solutions

Using the dimensionless stream functions $\psi$, $\psi=\Psi/aV_\infty$, velocity components are expressed as

$$v_r = \frac{1}{\xi}\frac{\partial\psi}{\partial\theta}, \quad v_\theta = -\frac{\partial\psi}{\partial\xi}$$

From the assumption of Eq. (8), $\psi$ can be expanded as follows,

$$\psi = \psi_0 + \alpha\psi_\alpha + \varepsilon_1\psi_\varepsilon + \cdots$$

### 2.1 Solution of Eq. (9)

Eq. (9) expressed in terms of $\psi_0$ is

$$\left[\frac{\partial^2}{\partial\xi^2} + \frac{1}{\xi}\frac{\partial}{\partial\xi} + \frac{1}{\xi^2}\frac{\partial^2}{\partial\theta^2}\right]^2\psi_0 = 0 \tag{13}$$

B. C. 1. $\dfrac{\partial\psi_0}{\partial\theta} = \dfrac{\partial\psi_0}{\partial\xi} = 0$, at $\xi = 1$ (14)

B. C. 2. $\psi_0 \to \xi\sin\theta$, as $\xi\to\infty$ (15)

Leaving Eq. (15) out of consideration, the solution for Eq. (13), which satisfies only Eq. (14) and diverges most slowly as $\xi$ increases, is obtained as follows[1],

$$\psi_0 = A\left[\xi\ln\xi - \frac{1}{2}\xi + \frac{1}{2}\xi^{-1}\right]\sin\theta \tag{16}$$

where $A$ is an undeterminate coefficient. Then the velocity components and pressure are given by

$$v_{r0} = A\left[\ln\xi - \frac{1}{2} + \frac{1}{2}\xi^{-2}\right]\cos\theta$$
$$v_{\theta 0} = -A\left[\ln\xi + \frac{1}{2} - \frac{1}{2}\xi^{-2}\right]\sin\theta$$
$$p_0 - p_\infty = -2A\xi^{-1}\cos\theta \tag{17}$$

On the other hand, Lamb's solution[3] for the Oseen equation can be expressed asymptotically in the region near the cylinder as follows[6],

$$\bar{\varPhi} \approx \frac{1}{B_0}\left[\xi \ln \xi - \frac{1}{2}\xi + \frac{1}{2}\xi^{-1}\right]\sin\theta \tag{18}$$

where $B_0=1/2-\gamma+\ln(8/Re)$, $\gamma$ is the Euler constant, 0.577⋯, and $Re=2aV_\infty/\nu$. Comparing Eq. (16) with Eq. (18), one can determine $A$ as follows,

$$A = \frac{1}{B_0} = \frac{1}{\frac{1}{2}-\gamma+\ln\frac{8}{Re}}, \qquad Re = \frac{2\rho_l V_\infty a}{\eta_1} \tag{19}$$

**2.2 Solution of Eq. (10)**

Using Eq. (16), Eq. (10) can be rewritten as follows,

$$\begin{aligned} 0 = &-\frac{\partial p_\alpha}{\partial \xi} + \left[\nabla^2 v_{r\alpha} - \frac{v_{r\alpha}}{\xi^2} - \frac{2}{\xi^2}\frac{\partial v_{\theta\alpha}}{\partial\theta}\right] \\ &+ \frac{1}{2B_0}[(4\xi^{-2}+3\xi^{-4}-26\xi^{-6}+48\xi^{-8}-24\xi^{-10})\cos\theta \\ &+ (\xi^{-4}-6\xi^{-6}+4\xi^{-8})\cos 3\theta] \\ 0 = &-\frac{1}{\xi}\frac{\partial p_\alpha}{\partial\theta} + \left[\nabla^2 v_{\theta\alpha} - \frac{v_{\theta\alpha}}{\xi^2} + \frac{2}{\xi^2}\frac{\partial v_{r\alpha}}{\partial\theta}\right] \\ &+ \frac{1}{2B_0}[(4\xi^{-2}-3\xi^{-4}+6\xi^{-6}-24\xi^{-10})\sin\theta \\ &+ (-3\xi^{-4}+6\xi^{-6}+4\xi^{-8})\sin 3\theta] \end{aligned} \tag{20}$$

Elimination $p_\alpha$ in Eq. (20) gives

$$\begin{aligned} \left[\frac{\partial^2}{\partial\xi^2} + \frac{1}{\xi}\frac{\partial}{\partial\xi} + \frac{1}{\xi^2}\frac{\partial^2}{\partial\theta^2}\right]^2 \psi_\alpha = &\frac{1}{B_0}[(6\xi^{-5}-28\xi^{-7} \\ &+ 24\xi^{-9}+96\xi^{-11})\sin\theta + (6\xi^{-5}-24\xi^{-7} \\ &- 8\xi^{-9})\sin 3\theta] \end{aligned} \tag{21}$$

$$\text{B. C. 1.} \quad \frac{\partial\psi_\alpha}{\partial\xi} = \frac{\partial\psi_\alpha}{\partial\theta} = 0, \quad \text{as } \xi = 1 \tag{22}$$

$$\text{B. C. 2.} \quad \psi_\alpha = o(\psi_0), \quad \text{as } \xi \to \infty \tag{23}$$

As mentioned previously, B. C. 2. is an approximate boundary condition. Assuming as a solution of Eq. (21) that

$$\psi_\alpha = \sum F_i(\xi)\Theta_i(\theta) \tag{24}$$

then,

$$\Theta_1 = \sin\theta, \quad \Theta_2 = \sin 3\theta \tag{25}$$

and differential equations for $F_1$ and $F_2$ become respectively

$$\begin{aligned} &\left[\frac{d^4}{d\xi^4} + \frac{2}{\xi}\frac{d^3}{d\xi^3} - \frac{3}{\xi^2}\frac{d^2}{d\xi^2} + \frac{3}{\xi^3}\frac{d}{d\xi} - \frac{3}{\xi^4}\right]F_1 \\ &= \frac{1}{B_0}(6\xi^{-5}-28\xi^{-7}+24\xi^{-9}+96\xi^{-11}) \end{aligned} \tag{26}$$

$$\begin{aligned} &\left[\frac{d^4}{d\xi^4} + \frac{2}{\xi}\frac{d^3}{d\xi^3} - \frac{19}{\xi^2}\frac{d^2}{d\xi^2} + \frac{19}{\xi^3}\frac{d}{d\xi} + \frac{45}{\xi^4}\right]F_2 \\ &= \frac{1}{B_0}(6\xi^{-5}-24\xi^{-7}-8\xi^{-9}) \end{aligned} \tag{27}$$

Solving these equations, $\psi_\alpha$, $v_{r\alpha}$, $v_{\theta\alpha}$ are obtained as follows,

$$\begin{aligned} \psi_\alpha = &\frac{1}{B_0}\Big[A_0^\alpha\xi^{-1}\ln\xi + \sum_{i=1}^{5} A_i^\alpha \xi^{-2i+3})\sin\theta \\ &+ (B_{-1}^\alpha\xi^{-3}\ln\xi + B_0^\alpha\xi^{-1}\ln\xi \\ &+ \sum_{i=1}^{3} B_i^\alpha\xi^{-2i+1})\sin 3\theta\Big] \end{aligned} \tag{28}$$

$$\begin{aligned} v_{r\alpha} = &\frac{1}{B_0}\Big[A_0^\alpha\xi^{-2}\ln\xi + \sum_{i=1}^{5} A_i^\alpha \xi^{-2i+2})\cos\theta \\ &+ 3(B_{-1}^\alpha\xi^{-4}\ln\xi + B_0^\alpha\xi^{-2}\ln\xi \\ &+ \sum_{i=1}^{3} B_i^\alpha\xi^{-2i})\cos 3\theta\Big] \end{aligned} \tag{29}$$

$$\begin{aligned} v_{\theta\alpha} = &\frac{1}{B_0}\Big[(C_0^\alpha\xi^{-2}\ln\xi + \sum_{i=1}^{5} C_i^\alpha \xi^{-2i+2})\sin\theta \\ &+ (D_{-1}^\alpha\xi^{-4}\ln\xi + D_0^\alpha\xi^{-2}\ln\xi \\ &+ \sum_{i=1}^{3} D_i^\alpha\xi^{-2i})\sin 3\theta\Big] \end{aligned} \tag{30}$$

Substituting these results into Eq. (20), $p_\alpha$ is given by

**Table 1** Coefficients of Eqs. (28), (29), (30), (31) and (32)

| $i$ | −1 | 0 | 1 | 2 | 3 | 4 | 5 |
|---|---|---|---|---|---|---|---|
| $A_i^\alpha$ | | −0.375 | 0.1584 | −0.0584 | −0.1458 | 0.02083 | 0.025 |
| $B_i^\alpha$ | 0.25 | 0.125 | −0.2 | 0.2125 | −0.0125 | | |
| $C_i^\alpha$ | | −0.375 | −0.1584 | 0.3166 | −0.4374 | 0.10415 | 0.175 |
| $D_i^\alpha$ | 0.75 | 0.125 | −0.325 | 0.3875 | −0.0625 | | |
| $E_i^\alpha$ | | | −2.0 | −0.75 | 2.833 | −3.5 | 1.20 |
| $G_i^\alpha$ | | 1.0 | −1.183 | 1.5 | −0.2 | | |

$$\begin{aligned} p_\alpha = &\frac{1}{B_0}\Big[\sum_{i=1}^{5} E_i^\alpha\xi^{-2i+1}\cos\theta + (G_0^\alpha\xi^{-3}\ln\xi \\ &+ \sum_{i=1}^{3} G_i^\alpha\xi^{-2i+1})\cos 3\theta\Big] \end{aligned} \tag{31}$$

Parameters in these equations are given in **Table 1**.

**2.3 Solution of Eq. (11)**

$\psi_\varepsilon$, $v_{r\varepsilon}$, and $v_{\theta\varepsilon}$ are obtained by multiplying $4/B_0^2$ to Eqs. (28), (29) and (30).

$$\begin{aligned} p_\varepsilon = &\frac{4}{B_0^3}\Big[\sum_{i=2}^{5} E_i^\varepsilon\xi^{-2i+1}\cos\theta + (G_0^\varepsilon\xi^{-3}\ln\xi \\ &+ \sum_{i=1}^{3} G_i^\varepsilon\xi^{-2i+1})\cos 3\theta\Big] \\ &E_i^\varepsilon = E_i^\alpha (i = 2, 3, 4, 5) \\ &G_i^\varepsilon = G_i^\alpha (i = 0, 1, 2, 3) \end{aligned} \tag{32}$$

## 3. Drag Force on a Cylinder

The distributions of the pressure and the rate-of-shear on a cylinder surface are given

$$\begin{aligned} P - P_\infty = &-\frac{\eta_1}{B_0}\frac{V_\infty}{a}\Big[2\cos\theta + \alpha(2.217\cos\theta \\ &- 0.117\cos 3\theta) + \frac{4\varepsilon_1}{B_0^2}(0.217\cos\theta \\ &- 0.117\cos 3\theta)\Big] \end{aligned} \tag{33}$$

$$\begin{aligned} 2D_{r\theta} = &-\frac{1}{B_0}\frac{V_\infty}{a}\Big[2\sin\theta + \left(\alpha + \frac{4\varepsilon_1}{B_0^2}\right)(1.283\sin\theta \\ &- 0.35\sin 3\theta\Big] \end{aligned} \tag{34}$$

The total drag $F$ per unit length of a cylinder is composed of the pressure drag $F_n$ and the friction drag $F_t$.

$$\begin{aligned} F_n &= a\int_0^{2\pi}(P_\infty - P)_{r=a}\cos\theta d\theta \\ &= \frac{2\pi V_\infty(1+\alpha)\eta_1}{B_0}[1+\delta_n] \\ \delta_n &= \frac{0.108\alpha + 0.433(\varepsilon_1/B_0^2)}{1+\alpha} \end{aligned} \tag{35}$$

$$\begin{aligned} F_t &= a\int_0^{2\pi}(-\tau_{r\theta})_{r=a}\sin\theta d\theta \\ &= \frac{2\pi V_\infty(1+\alpha)\eta_1}{B_0}[1-\delta_t], \quad \delta_t = \delta_n \end{aligned} \tag{36}$$

The total drag is given by

$$\begin{aligned} &F = F_t + F_n = \frac{4\pi V_\infty(1+\alpha)\eta_1}{B_0} \\ &\frac{1}{B_0} = \frac{1}{\frac{1}{2}-\gamma+\ln\frac{8}{Re}}, \qquad Re = \frac{2\rho_l V_\infty a}{\eta_1} \end{aligned} \tag{37}$$

This equation reduces to Lamb's equation[3] when $\alpha=\varepsilon_1=0$.

In Eqs. (35) and (36), $\delta_n$ and $\delta_t$ are parameters to represent the degree of deviation from the resistance law for Newtonian fluid due to the non-Newtonian viscosity. As is shown from these equations, they are the same in

Table 2 Parameters of Eq. (6)

| No. | Conc. [wt%] | Temp. [°C] | $\rho_l$ [g/cm³] | $\lambda_1^2\times10^4$ [sec²] | $\lambda_1^2\times10^3$ [sec²] | $\eta_1$ [g/cm·sec] | $\eta_2$ [g/cm·sec] |
|---|---|---|---|---|---|---|---|
| 1 | 2.16 | 30 | 1.006 | 2.19 | 50.0 | 4.50 | 0.856 |
| 2 | 2.48 | 25 | 1.009 | 2.69 | 25.9 | 8.71 | 2.66 |
| 3 | 2.87 | 35 | 1.005 | 1.62 | 85.3 | 8.19 | 3.50 |
| 4 | 2.93 | 35 | 1.007 | 1.27 | 3.55 | 4.02 | 0.944 |
| 5 | 3.19 | 35 | 1.009 | 7.77 | 116 | 13.4 | 2.24 |

magnitude and opposite in direction. As a consequence, the total drag exerted by a generalized Newtonian fluid is independent of the shear rate and determined only by the zero-shear viscosity. Of course, this result is applica ble only when the flow is very slow so that the condition of this analysis is satisfied.

For the case of a sphere[8], the friction drag is dominant over the pressure drag and consequently the total drag decreases. Taking the foregoing into consideration, it may be expected that the total drag increases when the pressure drag is dominant over the friction drag such as for the case of a disk.

## 4. Experiment

Small cylinders made of enameled copper were allowed to fall through aqueous solutions of C. M. C (Caboxymethyl celullose) contained in the tank of the dimension of 12×20×65 cm. Concentrations of C. M. C were 2.16, 2.48, 2.87, 2.93 and 3.19 weight percent. The cylinders used were 0.0473, 0.0630, 0.0733, 0.0837, 0.0940, 0.106 and 0.127 cm in diameter and 2, 3, 4, 5, 6 and 7 cm in

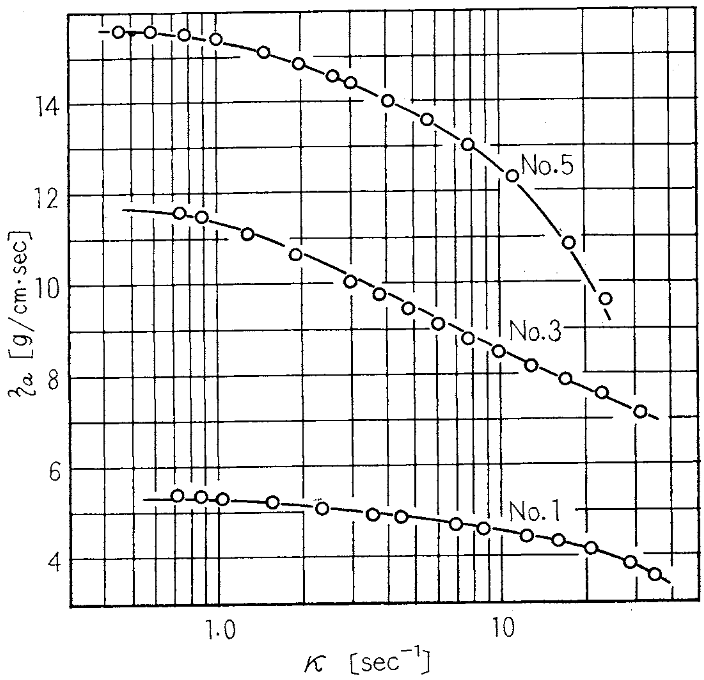


Fig. 1 Capillary viscometer data compared with Eq. (6)

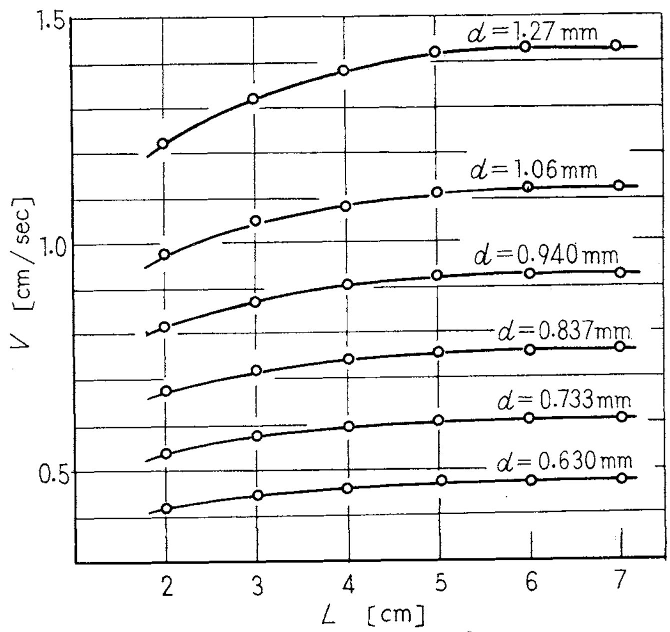


Fig. 2 Terminal velocities of cylinders as functions of their length, No. 5 solution, o; experimental points

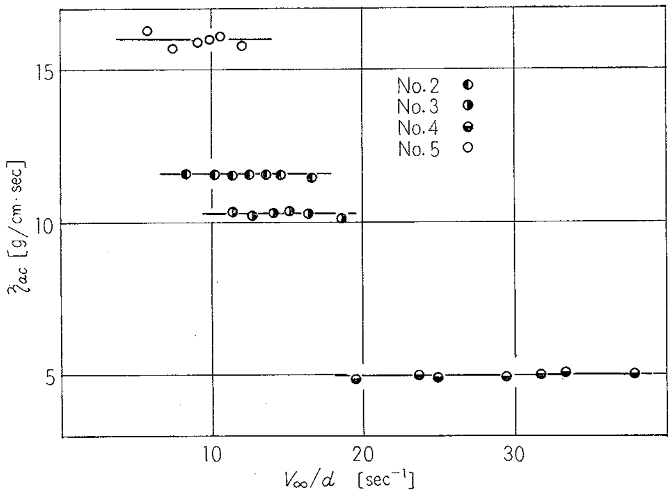


Fig. 3 Dependence of $\eta_{ac}$ on representative velocity gradient

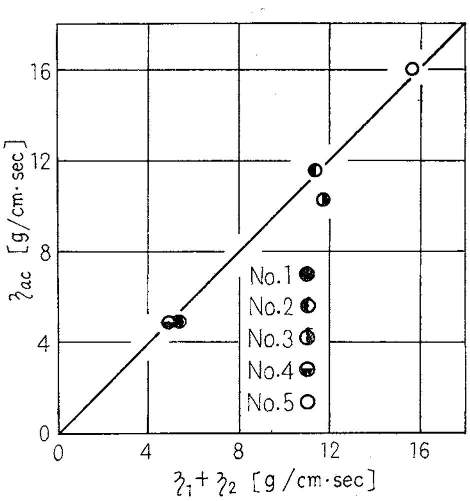


Fig. 4 Comparison of $\eta_{ac}$ with zero-shear viscosity, $\eta_1+\eta_2$

ength for each diameter. The density of the cylinder was approximately 8.00. A stopwatch was used for timing. Non-Newtonian viscosities were measured by the Maron, Krieger and Sisko capillary viscometer[4]. These data are shown in **Fig. 1**, where circles and solid lines represent measured and calculated values from Eq. (6) respectively. Parameters of Eq. (6), experimental temperature, and density of solutions are summarized in **Table 2**.

Since we are concerned with the two dimensional flow around a cylinder infinite in length, it is necessary to evaluate the possible end effects due to a finite-length cylinder. In order to eliminate these end effects, terminal velocities were measured on the cylinders of the same diameter but of the different length. If a cylinder is long enough so that end effects may be neglected, both the body force and the drag force on a cylinder increase in proportion to the length. Consequently, the terminal velocity should approach to a certain value. As an example, this is shown in **Fig. 2**. Since there is no reliable data of Newtonian fluid on the drag force on a cylinder at low Reynolds number at present, as a reference the same experiments were carried out for liquid jelly of various viscosities.

## 5. Results and Discussions

White showed that, on the contrary to the case where fluid is unbounded in extent, the wall effect is enormously large for the two dimensional flow so that the inertia effect may be neglected under usual experimental conditions. White's empirical formula[7] for the drag coefficient $C_D$ is expressed by

$$C_D = \frac{12.8}{Re \log\left(\frac{H}{d}\right)} \tag{38}$$

Where $H$ is the width between the walls. Also, Faxen's analytical result[2] is expressed as follows,

$$C_D = \frac{10.92}{Re \log\left(\frac{H}{d}\right) - 0.398} \tag{39}$$

The higher order terms of $H/d$ are neglected in Eq. (39).

On the other hand, our experimental data for liquid jelly were correlated within $\pm 5\%$ error by

$$C_D = \frac{9.44}{Re \log\left(\frac{H}{d}\right) - 0.660} \tag{40}$$

The experimental range of $H/d$ in Eq. (40) is from 94.3 to 254. In this range of $H/d$, the difference between Eq. (39) and Eq. (40) is within 3.6%. The prediction of Eq. (38) is relatively lower than that of Eq. (39).

Since in our experiment, geometrical parameters are the same for both solutions of C. M. C and liquid jelly, the data of C. M. C were analyzed on the base of Eq. (40). Taking the result of § 3 into consideration, we define an apparent viscosity $\eta_{ac}$ by the falling cylinder method as follows,

$$\eta_{ac} = \frac{C_D \log\left(\frac{H}{d}\right) - 0.660}{9.44} \rho_l V_\infty d \tag{41}$$

$\eta_{ac}$ is plotted against the representative velocity gradient $V_\infty/d$ in **Fig. 3**. This shows that it may be concluded that $\eta_{ac}$ is independent of $V_\infty/d$ in agreement with the result of § 3. **Fig. 4** is a plot of $\eta_{ac}$ vs. $(\eta_1+\eta_2)$. This shows that Eq. (41) predicts the zero-shear viscosity with good accuracy for $H/d$ ranging from 94.3 to 254.

For Newtonian fluid, the prediction of Lamb's equation is considerably lower than that of Faxen's equation at low

Reynolds number and the latter rather than the former explains experimental data under usual experimental conditions. By the same reason, the drag force itself does not agree with Eq. (37) quantitatively. However, the interesting result that the drag force (i. e., $\eta_{ac}$) is independent of $V_\infty/d$ and it can be determined only by the zero-shear viscosity is verified with good agreement. This result as well as that for a sphere[8] may be considered as an evidence for that it is useful for the creeping flow to assume a generalized Newtonian model. For the large value of $H/d$ where wall effects may be neglected, Eq. (37) is expected to predict the drag force quantitatively.

#### Acknowledgement

R. Nakamura acknowledges the financial support provided by the Sakkokai Foundation.

#### Nomenclature

| | | |
|---|---|---|
| $A$ | = undeterminate coefficient | [—] |
| $a$ | = radius of cylinder | [cm] |
| $B_0$ | = Eq. (18) | [—] |
| $C_D$ | = drag coefficient | [—] |
| $D_{ij}$ | = rate-of-deformation tensor | [sec$^{-1}$] |
| $d$ | = diameter of cylinder | [cm] |
| $F$ | = total drag per unit length of cylinder | [g·cm/sec$^2$] |
| $F_n$ | = pressure drag per unit length of cylinder | [g·cm/sec$^2$] |
| $F_t$ | = friction drag per unit length of cylinder | [g·cm/sec$^2$] |
| $H$ | = width between walls | [cm] |
| $h$ | = Eq. (7) | [—] |
| $P$ | = pressure | [g/cm·sec$^2$] |
| $p$ | = pressure, dimensionless | [—] |
| $r$ | = radial distance | [cm] |
| $Re$ | = Reynolds number | [—] |
| $V_\infty$ | = uniformly approaching velocity | [cm] |
| $V_i$ | = velocity vector | [cm] |
| $v_i$ | = velocity vector, dimensionless | [—] |
| $\alpha$ | = Eq. (6) | [—] |
| $\delta_n$, $\delta_t$ | = Eqs. (35) and (36) | [—] |
| $\varepsilon_i$ | = Eq. (6), $i=1, 2$ | [—] |
| $\eta_a$ | = apparent viscosity | [g/cm·sec] |
| $\eta_{ac}$ | = apparent viscosity by falling cylinder method, Eq. (41) | [g/cm·sec] |
| $\eta_1$, $\eta_2$ | = parameters of Eq. (6) | [g/cm·sec] |
| $\nu$ | = kinematic viscosity | [cm$^2$/sec] |
| $\xi$ | = radial distance, dimensionless | [—] |
| $\tau_{ij}$ | = stress tensor | [g/cm·sec$^2$] |
| $\Psi$ | = stream function | [cm$^2$/sec] |
| $\phi$ | = stream function, dimensionless | [—] |
| $\text{II}^*$ | = second invariant of rate-of-deformation tensor | [sec$^{-2}$] |
| $\text{II}$ | = second invariant of rate-of-deformation tensor, dimensionless | [—] |

#### Literature cited

1) Bretherton, F. P.: *J. Fluid Mech.*, **29**, 791 (1962)
2) Faxen, H.: *Proc. Roy. Swedish Inst. Engs. Res.* (*Stockholm*), **No. 187** (1964)
3) Lamb, H.: *"Hydrodynamics"*, Cambridge Univ. Press (1932)
4) Maron, S. H., Krieger, I. M. and Sisko, A. W.: *J. Appl. Phys.*, **25**, 8 (1954)
5) Oseen, C. W.: *"Hydrodynamik"*, Akad. Verlag, Leipzig (1927)
6) Proudman, I. and Pearson, J. R. A.: *J. Fluid Mech.*, **2**, 237 (1957)
7) White, L. M.: *Proc. Roy. Soc.* (London), **A 186**, 472 (1946)
8) Yoshioka, N. and Nakamura, R.: *Kagaku Kōgaku*, **29**, 791 (1965)

# STIMULUS AND RESPONSE OF GAS CONCENTRATION IN BUBBLING FLUIDIZED BEDS*

KUNIO YOSHIDA AND DAIZO KUNII
*Dept. of Chem. Eng., University of Tokyo, Tokyo*

## 1. Introduction

From the viewpoint of chemical reactors, it is important to investigate the characteristics of longitudinal gas dispersion. It is, however, generally difficult to predict the distribution of gas residence time in fluidized bed, because of the poor contact between gas and solids resulting from the formation of gas bubbles.

Kunii and Levenspiel[1] have proposed an idealized model of bubble behavior in the fluidized bed. This paper is concerned with the experimental and theoretical investigations on the stimulus response of the bubbling fluidized bed, based on the relations derived from the idealized model. In the present experiments, two kinds of gases, i. e., helium and Freon gas, were used as the tracer gas.

* Received on July 19, 1967

## 2. Basic Equations

### 2·1 Idealized model of bubbling bed

According to the idealized model of bubbling bed by Kunii and Levenspiel, the rising velocity of the bubble diameter are given respectively by the following equations.

$$u_b = u_0 - u_{mf} + 0.711(gd_b)^{1/2} \tag{1}$$

$$d_b = \frac{1.5}{n}(u_0 - u_{mf}) \tag{2}$$

Assuming the steady state operation, where the amount of solids transported upwards by the rising bubbles should be compensated by the amount of descending solids, the material balance of solids gives

$$(1 - \delta - \alpha\delta)u_s = \alpha\delta u_b \tag{3}$$

and from the gas balance,